Supporting Information

Optical and Electrical Properties of Perovskite Variant $(CH_3NH_3)_2SnI_6$

Fuji Funabiki[†], Yoshitake Toda[†], and Hideo Hosono[†]

[†]Materials Research Center for Element Strategy, Tokyo Institute of Technology, 4259 Nagatsuta, Yokohama 226-8503, Japan

S1. Crystal structures of $(CH_3NH_3)_2SnI_6$ powder and film

Rietveld refinements were conducted for $(CH_3NH_3)_2SnI_6$ in powder and film form. Eight CH_3NH_3 molecules oriented in the <111> direction were arranged in the double perovskite lattice, in which C and N were placed at 32f (0.2920, 0.2920, 0.2920) and 32f (0.2200, 0.2200, 0.2200), respectively, with an occupancy of 0.25. The results are shown in Figure S1 and Table S1. No impurity phases were detected. However, there was a slight difference in the structural data between the powder and the film. As the accuracy of the fitting was lower for the film, the structural data of the powder was used in this study.

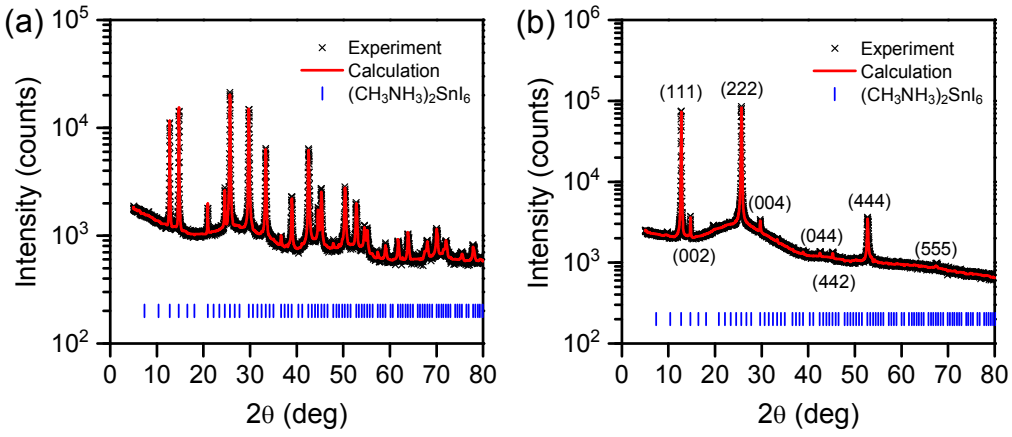

Figure S1. Rietveld refinements of the $(CH_3NH_3)_2SnI_6$ (a) powder and (b) film.

Table S1. Crystal Structure Parameters of the $(CH_3NH_3)_2SnI_6$ Powder and Film Determined from X-ray Diffraction Patterns at Room Temperature.

	powder	film
crystal system	cubic	cubic
space group	*Fm-3m*	*Fm-3m*
a (Å)	12.016(4)	12.025(6)
I: 24e (x, 0, 0)	0.2384(6)	0.2356(16)
R_{wp}	4.455	6.450

Sn: 4a (0, 0, 0). C: 32f (0.2920, 0.2920, 0.2920). N: 32f (0.2200, 0.2200, 0.2200).

S2. Effect of annealing on the lattice constant of the $(CH_3NH_3)_2SnI_6$ film

To elucidate the structural state of the $(CH_3NH_3)_2SnI_6$ film, the film was annealed in argon below the evaporation temperature. The results are shown in Figure S2. The lattice constant was slightly decreased by annealing. One possible reason is that the film may have been in a non-equilibrium state.

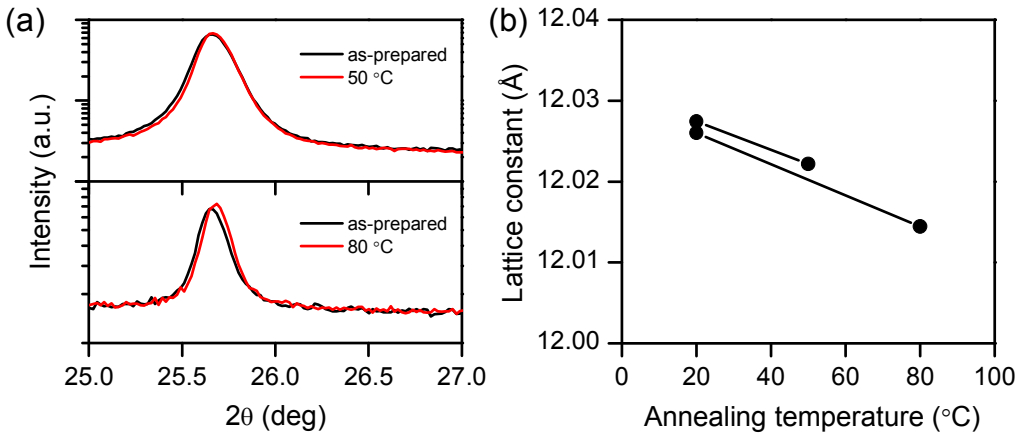

Figure S2. (a) X-ray diffraction peaks and (b) lattice constants of the $(CH_3NH_3)_2SnI_6$ films annealed in argon for 1 h.

S3. Crystal structure and absorption spectrum of Cs_2SnI_6

To compare the crystal parameters and band gap of $(CH_3NH_3)_2SnI_6$ with those of Cs_2SnI_6, the Cs_2SnI_6 powder was prepared by dry-mixing SnI_4 and CsI (99.999%, Sigma-Aldrich, USA), and the Cs_2SnI_6 film was deposited on a silica glass substrate by the thermal evaporation method. The results are shown in Table S3 and Figure S3.

Table S3. Crystal Structure Parameters of the Cs_2SnI_6 Powder Determined from X-ray Diffraction Pattern at Room Temperature.

crystal system	cubic
space group	*Fm-3m*
a (Å)	11.644
I: 24e (x, 0, 0)	0.2454
R_{wp}	5.904

Sn: 4a (0, 0, 0). Cs: 8c (1/4, 1/4, 1/4).

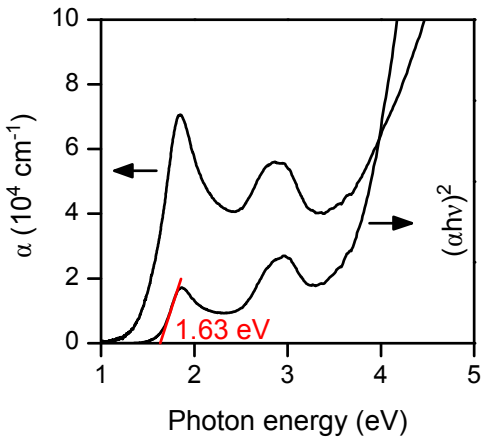

Figure S3. Absorption spectrum of the Cs_2SnI_6 film.

S4. Electrical properties of annealed $(CH_3NH_3)_2SnI_6$ films

To investigate the influence of grain boundaries, the $(CH_3NH_3)_2SnI_6$ film was annealed in argon below the evaporation temperature. Then, the electrical properties of the annealed films were measured at room temperature. The results are shown in Figure S4. There was no change in the grain size, but the grain shape clearly changed upon annealing. However, the carrier concentration, mobility, and photoconductivity remained unchanged irrespective of the annealing temperature.

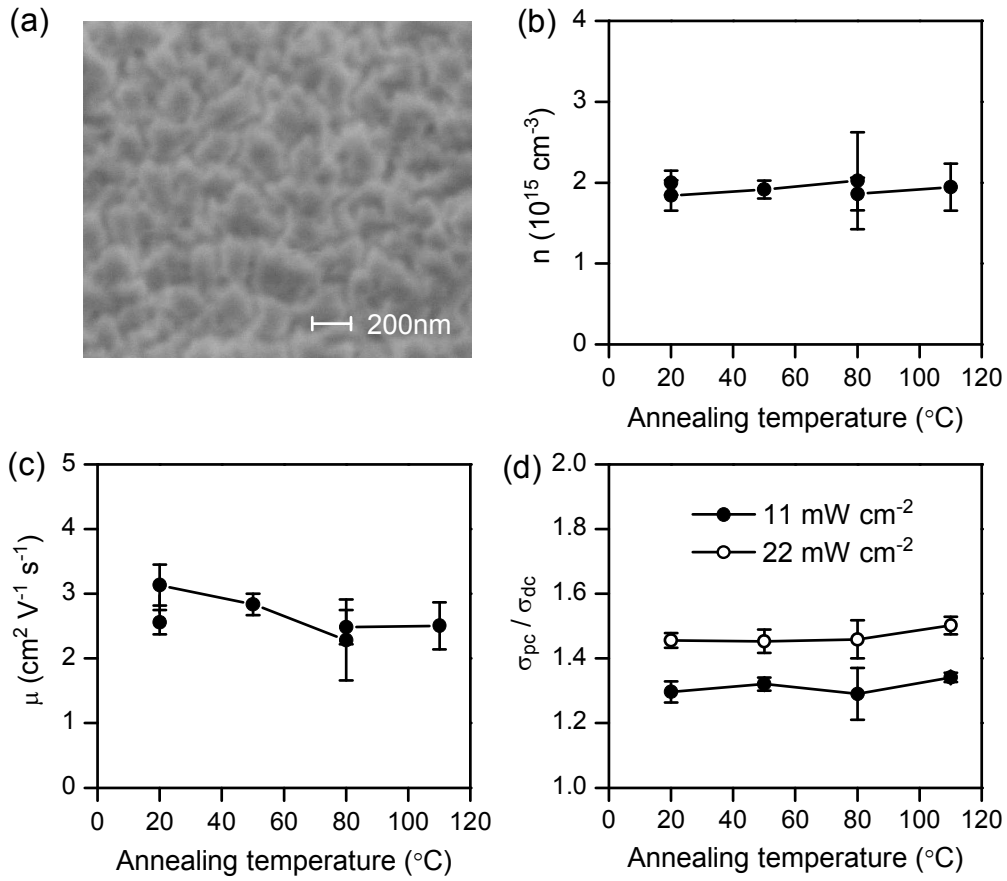

Figure S4. (a) Field emission scanning electron microscopy (FESEM) image of the $(CH_3NH_3)_2SnI_6$ film (300 nm thickness) annealed in argon at 110 °C for 1 h. (b) Room temperature carrier concentration and (c) mobility of the films annealed at different temperatures. (d) Photoconductivity divided by dark conductivity of the annealed films measured under simulated sunlight.